Kinetics of Transport of Dialkyloxacarbocyanines in Multidrug-Resistant Cell Lines Overexpressing P-glycoprotein: Interrelationship of Dye Alkyl Chain Length, Cellular Flux, and Drug Resistance†

Randy M. Wadkins‡ and Peter J. Houghton*

Department of Molecular Pharmacology, St. Jude Children's Research Hospital, 332 North Lauderdale, Memphis, Tennessee 38101

Received August 30, 1994; Revised Manuscript Received January 10, 1995⊗

ABSTRACT: The membrane transport properties of a series of dialkyloxacarbocyanine [$DiOC_n(3)$] dyes in multidrug-resistant KB cell lines were investigated to determine the influence of alkyl chain length on the ability of p-glycoprotein (i) to protect cells from the toxicity of the dyes and (ii) to affect the plasma membrane flux of the dyes. Cytotoxicity assays revealed that increased levels of p-glycoprotein led to increased resistance to the toxicity of the $DiOC_n(3)$ relative to the sensitive KB-3-1 parent line. This resistance could be fully or partially reversed by 10 μM verapamil. Monitoring of $DiOC_n(3)$ fluorescence changes allowed the measurement of accumulation and efflux rates for the dyes in the parent and two resistant cell lines at 1.5-s resolution. The flux of $DiOC_n(3)$ into and out of the KB85 and KBV1 cell lines was shown to be dramatically different from the parental KB-3-1 line when $n < 5$, while the transport properties of $n = 7$ were identical in the three cell lines examined. The membrane transport properties were shown not to be correlated with the 7-day toxicity of $DiOC_n(3)$. Verapamil affected the kinetic processes of $DiOC_{2-5}(3)$ involving redistribution of the dyes within the cells once they had initially passed the plasma membrane. Fluorescence microscopy was used to show no alteration in the subcellular distribution of the $DiOC_n(3)$, in response to neither chain length nor cell line. Our results indicate that an alkyl chain length of 5 carbons is the critical length necessary for p-glycoprotein to affect membrane transport of $DiOC_n(3)$ but not to protect the cells from the cytotoxicity of the dyes.

The phenomenon of p-glycoprotein- (pgp-)[1] mediated multidrug resistance (MDR) is one that has garnered considerable attention over the last few years [for reviews, see Endicott and Ling (1989), Ford and Hait (1990), and Tew et al. (1993)]. However, the mechanism by which pgp functions is still not fully understood. The most widely proposed model of the protein is one in which pgp "transports" or "pumps" toxic compounds from the interior of drug-resistant cell lines. This model has been developed on the basis of studies indicating ATP-dependent drug accumulation into inside-out membrane vesicles prepared from pgp-expressing cell lines (Horio et al., 1988, 1991). Such models of pgp require an interaction between pgp and its "substrate". Several studies on the ability of certain photoactivatable analogs of antitumor drugs and/or MDR modulators to selectively photolabel pgp suggest that direct drug binding to pgp may occur [reviewed in Beck and Qian (1992)].

One curious aspect of MDR cells is that there is no obvious structure−activity relationship among the variety of compounds thought to interact with pgp [e.g., Ford and Hait (1990)]. One rationale for this may be the variety of ways in which both antitumor drugs and MDR-modulating drugs interact with MDR cells. Recent work from our laboratory (Wadkins & Houghton, 1993) has shown that potent MDR modulators may interact with either pgp or the plasma or organelle membranes of pgp-expressing cells and may therefore be involved in many mechanisms of action.

Another problem with assessing structure−activity relationships for pgp substrates is the lack of good model compounds with which to work. Derivatization of antitumor drugs and other pharmacological agents often results in production of compounds with much different physical properties than those of the original compound of interest, while examination of agents having diverse structural composition yields unsatisfying results [e.g., Klopman et al. (1992)].

Recently, studies using a more reductionist approach to determine what constitutes a pgp-"binding" compound have been performed. Gros et al. (1992) have shown that simple lipophilic phosphonium and arsonium derivatives are part of the MDR phenotype in *mdr1* transfected murine cell lines. Work from Lampidis and co-workers (Dellinger et al., 1992) has provided the most detailed analysis of simple structural modifications on the ability of pgp expression to confer resistance. Using alkylpyridiniums and alkylguanidiniums with increasing alkyl chain lengths, it was found that resistance to cytotoxicity in pgp+ cells increased with increasing chain length in the alkylpyridiniums but not in alkylguanidiniums, suggesting (i) that a delocalized ring system is important for pgp recognition and (ii) that a critical

† This work was supported by USPHS Awards CA 23099 and CA 51949 and Cancer Center Support (CORE) Grant CA 21765 from the National Cancer Institute and American Lebanese Syrian Associated Charities (ALSAC).

* To whom correspondence and reprint requests should be addressed [Fax (901)-521-1668].

‡ Present address: Code 6900, Naval Research Laboratory, Washington, DC 20375 (e-mail rwadkins@cbmse.nrl.navy.mil).

⊗ Abstract published in *Advance ACS Abstracts,* March 1, 1995.

[1] Abbreviations: pgp, p-glycoprotein; MDR, multidrug resistance; $DiOC_n(3)$, dialkyloxacarbocyanine iodide; KB31, KB-3-1 HeLa cells; KB85, KB-Ch^R-8-5 HeLa cells; KBV1, KB-V-1 HeLa cells; FDIM, fluorescence digital imaging microscopy; DOX, doxorubicin; VCR, vincristine.

0006-2960/95/0434-3858$09.00/0

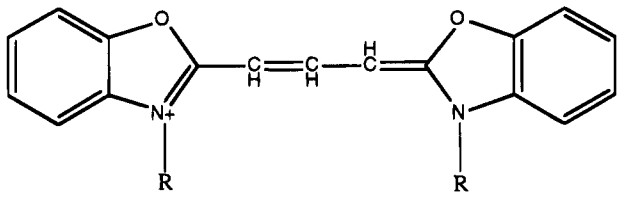

R	Dye
$-CH_2CH_3$	$DiOC_2(3)$
$-(CH_2)_2CH_3$	$DiOC_3(3)$
$-(CH_2)_4CH_3$	$DiOC_5(3)$
$-(CH_2)_5CH_3$	$DiOC_6(3)$
$-(CH_2)_6CH_3$	$DiOC_7(3)$

FIGURE 1: Chemical structure of the $DiOC_n(3)$ dyes used in this study. Iodide was the counterion.

alkyl tail length of ca. 5 carbons is necessary to be recognized by pgp.

Another controversial question in pgp-mediated resistance is whether pgp acts to efflux drugs or, instead, to prevent their initial accumulation. Most studies with a variety of pgp-expressing cell lines and antitumor drugs have reported enhanced efflux of total drug from MDR cells versus drug-sensitive cell lines when cells are loaded to similar initial drug levels. This is primarily due to the fact that efflux of hydrophobic drugs is usually a much slower process than accumulation and is therefore more easily measured without the need for specialized equipment.

In some cases, substantially reduced rates of influx of drugs into MDR cells have been reported, even when little or no alteration in efflux is observed. Sirotnak et al. (1986) reported decreased vincristine (VCR) influx into MDR cells with little change in VCR efflux, as have Stow and Warr (1993) in a similar study. The Sirotnak et al. studies concluded that their MDR cell lines showed similar doxorubicin (DOX) influx but slightly increased DOX efflux. Ramu et al. (1989) showed that MDR lines had greatly reduced DOX influx and suggested that the active efflux model for pgp action was not necessary to explain the mechanism of drug resistance. More recently, Roepe (1992) has shown that, when loaded to identical drug levels, MDR cells do efflux slightly more (35%) DOX than their sensitive counterparts but that the initial rates of efflux are identical in the sensitive and MDR lines. Furthermore, recent work by Shalinsky et al. (1993) has shown that, even within the initial 20 s of incubation, pgp-expressing cells show greatly reduced vinblastine influx, suggesting that pgp function is a virtually immediate process. A similar conclusion has been reached by Stein et al. (1994) for accumulation of colchicine, vinblastine, and VP-16 into MDR cells. Thus, the question as to whether pgp acts to reduce influx, enhance efflux, or both, has not been unambiguously ascertained.

In the studies described here, we have utilized the fluorescence properties of the dialkyloxacarbocyanine dyes [$DiOC_n(3)$; Figure 1] to address three fundamental questions concerning pgp action described above: (i) what are the structural requirements for a compound to be recognized by pgp, (ii) how does the presence of pgp affect the transmembrane flux of the compounds it protects the cell from, and (iii) how do pgp modulators affect both the transmembrane flux of $DiOC_n(3)$ and their toxicity? Earlier work using $DiOC_2(3)$, $DiOC_5(3)$, and $DiOC_6(3)$ has shown that these dyes are part of the pgp-mediated MDR phenotype (Chaudhary & Roninson, 1991; Crifo et al., 1991; Horton et al., 1990). The $DiOC_n(3)$ dyes have several advantages over drugs such as DOX or VCR, in that they are permanent cations (pK_a > 10) and their protonation state is unaffected by extra- or intracellular pH differentials; they are highly fluorescent and can be used in the nanomolar range rather than the micromolar range (often used for DOX studies); their fluorescence is enhanced upon cellular accumulation, and thus an increasing signal is measured, in contrast to DOX, which shows a decreased signal upon cellular accumulation; and the fluorescent ring system of the $DiOC_n(3)$ is generally unaffected by altering the alkyl chain length of the dyes (Sims et al., 1974), and thus the physical properties of the dyes can be determined by the length of the dye's carbon "tail". These properties make this series of dyes a valuable tool in determining the mechanism of pgp action. We report here the dependence of pgp-mediated MDR on $DiOC_n(3)$ tail length and measure both the immediate accumulation and efflux kinetics of dye transport. Further, we report the effect of verapamil, a potent inhibitor of pgp function, on both the kinetics of transmembrane $DiOC_n(3)$ flux and the toxicity of the $DiOC_n(3)$ to KB cells.

MATERIALS AND METHODS

Chemicals and Cell Lines. 3,3′-Diethyloxacarbocyanine iodide [$DiOC_2(3)$] and 3,3′-dipropyloxacarbocyanine iodide [$DiOC_3(3)$] were obtained from Aldrich Chemical Co. (Milwaukee, WI). 3,3′-Dipentyloxacarbocyanine iodide [$DiOC_5(3)$] and 3,3′-diheptyloxacarbocyanine iodide [$DiOC_7(3)$] were obtained from Molecular Probes (Eugene, OR). 3,3′-Dihexyloxacarbocyanine iodide [$DiOC_6(3)$] was obtained from Eastman Laboratory Chemicals (Rochester, NY). Non-enzymatic cell dissociation solution was obtained from Sigma (St. Louis, MO).

Accumulation and efflux kinetics both in the spectrometer and under the microscope were performed in β-buffer: 15 mM β-glycerophosphate, 150 mM NaCl, 10 mM glucose, 0.5 mM $MgCl_2$, 1.8 mM $CaCl_2$, and 3 mM $KHCO_3$, adjusted to pH 7.4.

The human cervical carcinoma derived KB-3-1 (KB31) cell lines, the colchicine selected KB-Ch^R-8-5 (KB85) lines, and the vinblastine selected KB-V-1 (KBV1) cell lines were the generous gift of Dr. M. Gottesman (NIH, Washington, DC). These cell lines, which show increasing levels of p-glycoprotein and (for KB85 and KBV1) express the multidrug resistance phenotype, have been characterized elsewhere (Shen et al., 1986). The cell lines were grown in monolayer cultures at 37 °C in 10% CO_2 atmosphere incubators in antibiotic-free DMEM supplemented with 10% bovine serum albumin and 4 mM L-glutamine. The KB85 line was grown in the continual presence of 10 ng/mL colchicine (Sigma Chemical Co., St. Louis, MO) while the KBV1 line was grown in 1 μg/mL vinblastine sulfate (Cetus Corp., Emeryville, CA).

Cytotoxicity Assays. Colony formation assays were used to determine the toxicity of the $DiOC_n(3)$ to the three KB

cell lines. Cells were plated in triplicate at a density of 3000 cells/well in Falcon six-well flat-bottom tissue culture plates (Becton Dickson Co., Lincoln Park, NJ). After 24 h, the incubation media were replaced with 3 mL of fresh media containing 0.001−100 μM of DiOC$_n$(3), and cells were incubated for 7 days further. The media were aspirated and cells washed once with 2 mL of 0.9% saline and dried overnight. Colonies were stained with 1 mL of 0.1% crystal violet (Fluka, Ronkonkoma, NY) and washed twice with distilled water. Colonies were counted using an ARTEK Model 880 colony counter. The IC_{50} values were defined as the concentration of DiOC$_n$(3) producing 50% of the colonies found in control wells containing no DiOC$_n$(3).

Accumulation Studies. Cells in log-phase growth were harvested from a single well of a Falcon six-well plate by incubating the cells for 2 min with 1 mL of nonenzymatic cell dissociation solution (Sigma, St. Louis, MO). The cells were subsequently triturated, suspended in β-buffer, and used immediately. To monitor accumulation kinetics, 200 μL of a 3.0×10^6 cell/mL solution was mixed in a polymethacrylate cuvette (Sigma), mounted in a Perkin-Elmer LS-5 fluorescence spectrometer and containing 2 mL of β-buffer and various concentrations of DiOC$_n$(3). The fluorescence from the continually stirred cell−DiOC$_n$(3) suspension was monitored using an Apple IIGS microcomputer equipped with a data acquisition card connected to the chart recorder output of the spectrometer. Data were collected in 1.5-s intervals for DiOC$_{5-7}$(3) and in 5-s intervals for DiOC$_{2-3}$(3). Concentration of DiOC$_n$(3) within cells resulted in enhanced fluorescence at 509 nm (8-nm slits) that could be monitored using 484-nm excitation (4−8-nm slits). These wavelengths correspond to the excitation and emission maxima for the DiOC$_n$(3), respectively. Note that the fluorescence increase observed at low concentrations with DiOC$_n$(3) is in contrast to the decrease in fluorescence observed with other classes of cyanine dyes [see, e.g., Seligmann and Gallin (1983)]. Experiments were performed at ambient temperature (23 ± 1 °C).

Averaged accumulation curves are shown in Figure 2. These curves exhibited behavior typical for multicompartmental flux. In general, after several scenarios were tested for dye signal, the simplest model that could effectively fit the accumulation of all the DiOC$_n$(3) was a superposition of two processes:

$$A \rightarrow B \rightarrow C \qquad \text{(process 1)}$$

with an additional term for

$$D \rightarrow E \qquad \text{(process 2)}$$

where increased fluorescence is primarily due to the presence of dye in compartments B and E, with B having the highest contribution to the observed signal. This model leads to the differential equations that describe the fluorescence signal F [see, e.g., Moore and Pearson (1981)]:

$$\frac{dF}{dt} = \frac{dB}{dt} + \frac{dE}{dt} = k_1A - k_2B + k_3E \qquad (1)$$

In our case, we are measuring heterogeneous signals, and so the parameters A, B, C, D, and E represent fluorescence intensities that are proportional to concentrations but do not provide information as to the concentrations themselves.

Using Laplace transforms, the differential equations can be solved to yield a fitting equation that describes the fluorescence signal F observed

$$F = \frac{k_1A_1}{k_2 - k_1}(e^{-k_1t} - e^{-k_2t}) + A_2(1 - e^{-k_3t}) + F_o \qquad (2)$$

where the k's represent effective rate constants and A_1, A_2, and F_o represent amplitudes for the signals arising from process 1, process 2, and background or initial fluorescence, respectively. Upon initial fitting of the data, it became clear that in many instances the best fits were obtained when $k_2 \approx k_1$. Therefore, the fitting equation could be further simplified to

$$F = A_1k_1te^{-k_1t} + A_2(1 - e^{-k_3t}) + F_o \qquad (3)$$

where the parameters are as described above. Equation 2 or 3 or a portion thereof (see Results and Table 2) was used to fit each accumulation data set using nonlinear least squares fitting routines (Kaleidagraph, Synergy Software, Reading, PA). It should be stressed that the equations and model fit the accumulation curves, but there may be other models that could also represent these curves. Our model represents the minimal model needed to effectively fit the data. Also, the values of A and k can be concentration dependent. Thus, the parameters derived here should only be used comparatively to characterize the flux properties of a given concentration of dye in the three KB cell lines. The nature of the compartments B−E is unknown, but on the basis of the fluorescence microscopy data given below, we suggest A is an extracellular dye, B is the plasma or mitochondrial membrane, and C is an aggregated state within the mitochondria. Such a model has been reported elsewhere for accumulation of other dyes within mitochondria [see, e.g., Bunting et al. (1989) and Bunting (1992)]. The D and E compartments may be either a second mitochondrial or plasma membrane state but appear to be due to intracellular trafficking of dye. We have interpreted the effect of pgp expression and the presence of verapamil on the flux of DiOC$_n$(3) according to this model.

The total amount of DiOC$_n$(3) could be determined by pelleting of the cells following incubation with dye. At the end of the accumulation studies described above, the cuvettes containing dye and cells were placed in a Beckman Accuspin FR centrifuge at 4 °C and spun at 400g for 5 min. The supernatant was aspirated, and the subsequent pellet was mixed with 2 mL of methanol to solubilize cell-bound dye. The fluorescence of the methanol solution was compared to a standard curve to determine the total amount of DiOC$_n$(3) contained in the cells.

Efflux Studies. Following accumulation, the cells were pelleted as described above. The pellet was then resuspended in 2 mL of dye-free β-buffer and the cuvette returned to the holder in the spectrometer. The fluorescence signal was monitored with time as for the accumulation studies. Data were collected at 5-s intervals for DiOC$_{5-7}$(3) and at 10-s intervals for DiOC$_{2-3}$(3).

Fluorescence Digital Imaging Microscopy. For the microscopy experiments, the sample preparation method described by McKenna and Wang (1989) was used. KB31 or KB85 cells were plated onto no. 1, 48 × 60 mm glass coverslips (Thomas Scientific) that had been secured to the bottom of plexiglass chambers with Dow Corning high-vacuum grease. The cells were allowed to attach to the plates for 48 h. The chamber was then mounted onto the stage of a Zeiss Axiovert 135TV inverted microscope and a field of

Table 1: Cytotoxicity of $DiOC_n(3)$ Derivatives in KB Cell Lines after 7 Days of Continuous Exposure[a]

	IC_{50} (μM)				
derivative	KB31	KB85	fold resistance[b]	KBV1	fold resistance[a]
$DiOC_2(3)$	0.05 ± 0.01	1.10 ± 0.50	22.0	3.65 ± 0.88	73.0
$DiOC_3(3)$	0.04 ± 0.00	0.35 ± 0.04	8.8	2.44 ± 0.48	61.0
$DiOC_5(3)$	0.04 ± 0.01	0.40 ± 0.04	10.0	2.46 ± 0.37	61.5
$DiOC_6(3)$	0.04 ± 0.00	0.40 ± 0.06	10.0	2.65 ± 0.10	66.3
$DiOC_7(3)$	0.05 ± 0.01	0.35 ± 0.03	7.0	2.09 ± 0.10	41.8

[a] Data given are the average ± standard deviation for at least three determinations performed in triplicate. [b] Relative to the sensitive KB31 line.

cells observed with a 63× Plan-Neofluar oil immersion objective.

A solution of β-buffer containing 10 nM $DiOC_2(3)$ or $DiOC_6(3)$ was introduced into the chamber, and the fluorescence from a field of cells was monitored using a Photometrics CE200A digital charge-coupled device camera with a 1K × 1K pixel array. A Xe lamp source was used, with excitation at 485 ± 10 nm and emission detected at 520−560 nm. Digital images were obtained at various times using a 5-s exposure and were transferred to a Silicon Graphics Crimson/XS computer for analysis. Quantitation of the images was peformed by subtracting a background equal to the total area of the cell image with an average intensity corresponding to regions of the original image not containing stained cells. The total remaining fluorescence signal was then integrated. Subsequent to integration, the images were filtered using a 3 × 3 highpass digital image sharpening filter to highlight details of dye distribution. Experiments were performed at ambient temperature (23 ± 1 °C).

RESULTS

Cytotoxicity of $DiOC_n(3)$ Dyes. The ability of $DiOC_n(3)$ dyes to inhibit growth of KB cells was tested using 7-day colony formation assays. The results of this assay are presented in Table 1. Although all cell lines were slightly more resistant to the toxicity of $DiOC_2(3)$, in general the toxicity of the dyes was not correlated with dye alkyl chain length. The pgp-expressing KB85 cells were 7−22-fold more resistant to the $DiOC_{2-7}(3)$ than their parent KB31 cells. The KBV1 cells were highly resistant to the toxic effects of $DiOC_n(3)$ as compared to their sensitive KB31 parents: from 42- to 72-fold. Thus, both pgp-expressing KB85 and KBV1 cell lines exhibit marked resistance to $DiOC_n(3)$.

Kinetics of $DiOC_n(3)$ Accumulation in Sensitive and Resistant Cell Lines. To test whether the resistance of pgp-expressing cells was due to alterations in the influx rates of the dyes, as has been implicated in resistance to *vinca* alkaloids and anthracyclines (Sirotnak et al., 1986; Ramu et al., 1989; Stow & Warr, 1993; Shalinsky et al., 1993), we measured the fluorescence increase as $DiOC_n(3)$ entered the KB cells. The fluorescence with respect to time is plotted in Figure 2 for the $DiOC_n(3)$ in the three KB cell lines.

Each $DiOC_n(3)$ had its own characteristic accumulation profile, suggesting different intracellular interactions. Accumulation of all $DiOC_n(3)$ exhibited an initial fast binding of the dyes followed by a slower binding and/or redistribution. The general shape of the accumulation curves remained constant at either 360 or 180 nM external dye concentration, as well as for higher and lower concentrations (data not shown). However, the rate parameters (effective rate constants and relative amplitudes) were not always independent of the external dye concentration (Table 2), as has also been observed with isolated mitochondria systems (Bunting, 1992).

For $DiOC_7(3)$ the accumulation profiles remained essentially identical among the KB cell lines, with the only variation being a slight alteration in the amplitude of process 2 for KB85. The values for k_2 are highly dependent on external dye concentration, increasing approximately 10-fold with a doubling of external concentration. Furthermore, it was unecessary to use process 2 in the fits at low (180 nM) external concentrations, and therefore process 1 provided an acceptable description of $DiOC_7(3)$ dye accumulation. The rate constant k_1 showed only a slight dependence on external dye concentration, while the amplitude for process 1 was approximately proportional to external dye concentration. These results support our assumptions that the $A \rightarrow B$ step of process 1 is an external → internal movement, while the other steps represent intracellular redistributions of dye.

The accumulation of $DiOC_6(3)$ is almost identical between KB31 and KB85 cell lines, and thus the presence of moderate amounts of pgp does not significantly affect the influx of this dye. There is a slight decrease in the amplitudes of the signal changes for $DiOC_6(3)$ accumulation as one progresses from KB31 to KBV1. The most pronounced difference among cell lines occurs at 180 nM external dye, where the contribution of process 2 to the accumulation profile is considerable in the KBV1 line. Also, in KBV1, process 2 has an amplitude of similar magnitude to that for process 1. These data indicate that the membrane flux of $DiOC_6(3)$ is at least partially affected by the presence of high levels of pgp.

In contrast to $DiOC_7(3)$ and $DiOC_6(3)$, accumulation of $DiOC_5(3)$ was noticeably different in the three cell lines examined. The parameters for the $B \rightarrow C$ component of process 1 were the most affected by the presence of pgp. The rate constant k_2 for this process is enhanced approximately 3-fold in KB85 but virtually eliminated in KBV1 (reduced 600-fold for 360 nM external dye or eliminated for 180 nM external dye). The magnitude of the signal change accompanying $DiOC_5(3)$ accumulation was also inversely proportional to cellular pgp content. KBV1 cells that highly express pgp showed a $DiOC_5(3)$ signal change of about one-third of that for the drug-sensitive KB31 cell line, and KB85 cells, which express moderate amounts of pgp, gave approximately two-thirds of the signal change occurring with the sensitive line.

Accumulation of $DiOC_3(3)$ into KB31 and KB85 is characterized by surprisingly similar rate constants for all processes involved (Table 2), indicating that the difficulty associated with penetration of the plasma membrane for $DiOC_3(3)$ is the same in the two cell lines, irrespective of the presence of pgp. The primary distinction between the two lines is the significantly decreased amplitude for

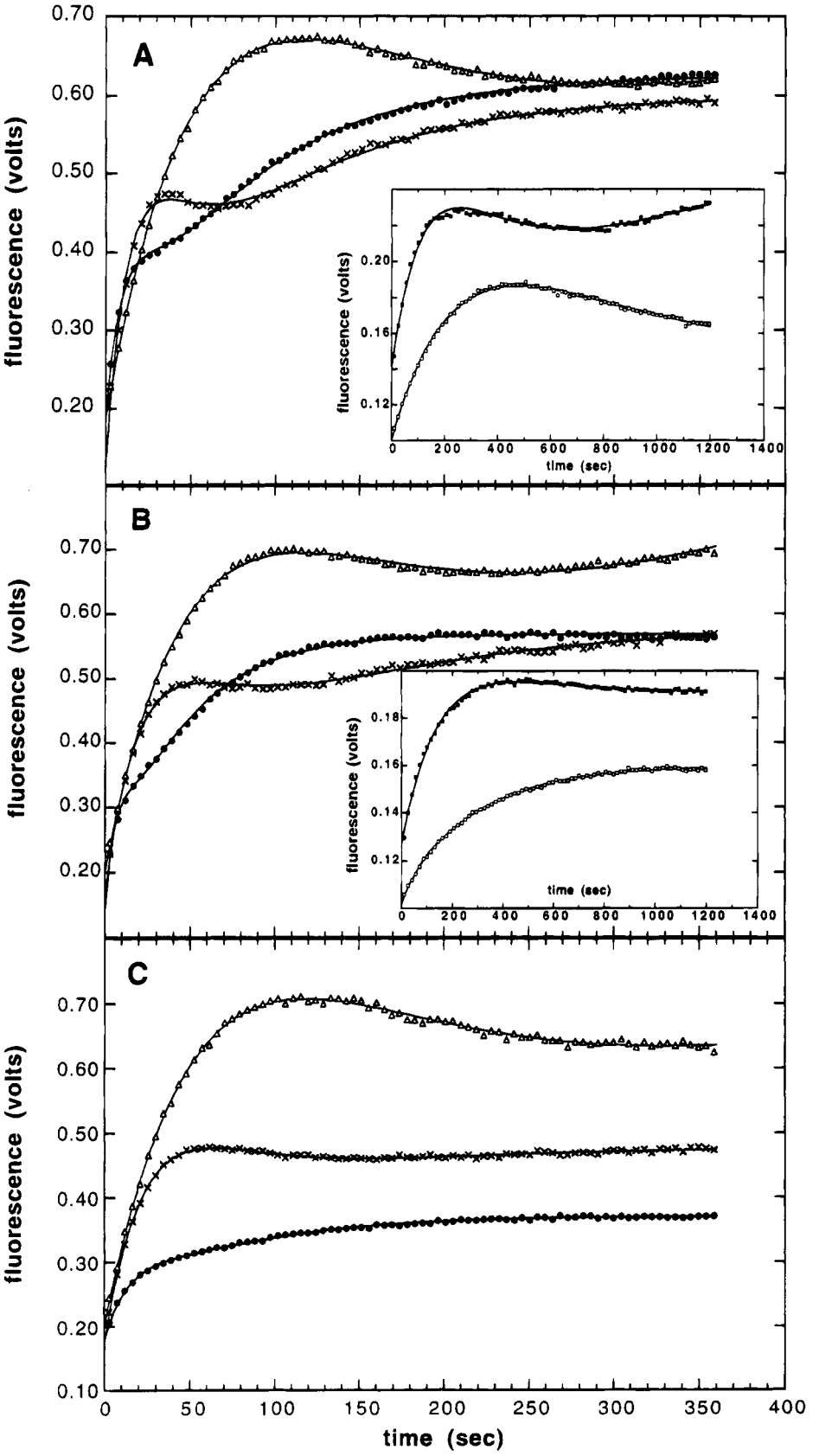

FIGURE 2: Accumulation of $DiOC_n(3)$ into KB cell lines. For clarity of presentation, only every third data point is plotted for $DiOC_{5-7}(3)$, while every other data point is plotted for $DiOC_{2-3}(3)$. Solid lines represent curve fits to eq 2 or 3 in Materials and Methods. The resulting parameters are recorded in Table 2. Plots are the average of at least three transients and show accumulation of 360 nM external $DiOC_7(3)$ (△), $DiOC_6(3)$ (×), $DiOC_5(3)$ (●), $DiOC_3(3)$ (■), and $DiOC_2(3)$ (□) into 3×10^5 cells/mL (A) KB31, (B) KB85, and (C) KBV1 cells. Increasing fluorescent intensity corresponds to increased voltage.

accumulation into KB85. Thus, KB85 accumulates only about 40% of the $DiOC_3(3)$ taken up by KB31. The amplitudes for the entry of $DiOC_3(3)$ into KB31 are similar at both 360 and 180 nM external dye concentrations, as is that for KB85, suggesting that accumulation of $DiOC_3(3)$ may be a saturable process.

Table 2: Kinetic Parameters for Cellular $DiOC_n(3)$ Accumulation[a]

dye	cell line	external concn (nM)	A_1 (relative)	$k_1 \times 10^4$ (s^{-1})	$k_2 \times 10^4$ (s^{-1})	A_2 (relative)	$k_3 \times 10^4$ (s^{-1})
$DiOC_7(3)$	KB31	360	0.97 ± 0.14	123 ± 24	123 ± 24	0.68 ± 0.04	23 ± 2
		360 + VRP[b]	0.82 ± 0.01	113 ± 1	113 ± 1	1.25 ± 0.29	8 ± 2
		180	0.43 ± 0.01	175 ± 2	15 ± 0	–[c]	–
	KB85	360	1.00 ± 0.09	122 ± 12	122 ● 12	1.51 ± 0.23	10 ± 2
		360 + VRP[b]	0.49 ± 0.02	130 ± 4	130 ± 4	0.41 ± 0.01	57 ± 6
		180	0.40 ± 0.00	200 ± 2	13 ± 0	–	–
	KBV1	360	1.00 ± 0.03	115 ± 8	115 ± 8	0.63 ± 0.05	26 ± 7
		360 +VRP[b]	0.81 ± 0.01	89 ± 1	89 ± 1	0.84 ± 0.05	12 ± 3
		180	0.35 ± 0.00	187 ± 2	10 ± 0	–	–
$DiOC_6(3)$	KB31	360	0.57 ± 0.01	481 ± 4	481 ± 4	0.48 ± 0.00	121 ± 1
		180	0.19 ± 0.00	595 ± 6	4 ± 1	–	–
	KB85	360	0.53 ± 0.01	356 ± 3	356 ± 3	0.45 ± 0.00	119 ± 1
		180	0.26 ± 0.00	485 ± 5	1 ± 1	–	–
	KBV1	360	0.45 ± 0.03	289 ± 7	289 ± 7	0.31 ± 0.02	133 ± 14
		180	0.17 ± 0.02	290 ± 4	290 ± 4	0.15 ± 0.01	154 ± 6
$DiOC_5(3)$	KB31	360	0.20 ± 0.00	1550 ± 78	374 ± 14	0.46 ± 0.00	135 ± 1
		360 + VRP[b]	0.20 ± 0.00	1406 ± 56	185 ± 6	0.43 ± 0.00	73 ± 1
		180	0.14 ± 0.00	1196 ± 68	221 ± 14	0.27 ± 0.00	130 ± 3
	KB85	360	0.23 ± 0.01	1265 ± 23	1265 ± 23	0.44 ± 0.00	241 ± 2
		360 + VRP[b]	0.20 ± 0.00	1222 ± 40	96 ± 5	0.46 ± 0.01	39 ± 2
		180	0.17 ± 0.02	1205 ± 48	1205 ± 48	0.31 ± 0.01	221 ± 4
	KBV1	360	0.10 ± 0.00	1290 ± 49	2 ± 1	0.12 ± 0.00	109 ± 5
		360 + VRP[b]	0.16 ± 0.00	680 ± 29	–	0.12 ± 0.00	133 ± 5
		180	0.04 ± 0.00	657 ± 212	–	0.06 ± 0.01	91 ± 24
$DiOC_3(3)$	KB31	360	0.18 ± 0.02	55 ± 3	55 ± 3	0.13 ± 0.04	9 ± 5
		360 + VRP[b]	0.09 ± 0.00	429 ± 20	54 ± 2	0.16 ± 0.00	16 ± 0
		180	0.19 ± 0.04	35 ± 3	35 ± 3	0.13 ± 0.05	18 ± 2
	KB85	360	0.07 ± 0.04	55 ± 3	55 ± 3	0.13 ± 0.04	9 ± 5
		360 + VRP[b]	0.11 ± 0.00	283 ± 7	31 ± 1	0.13 ± 0.01	6 ± 1
		180	0.05 ± 0.02	47 ± 16	47 ± 16	0.06 ± 0.01	26 ± 11
	KBV1	360 + VRP[b]	0.06 ± 0.00	111 ± 2	2 ± 0	–	–
$DiOC_2(3)$	KB31	360	0.12 ± 0.00	48 ± 1	6 ± 0	–	–
		360 + VRP[b]	0.09 ± 0.00	36 ± 1	36 ± 1	0.03 ± 0.00	78 ± 7
		180	0.07 ± 0.00	67 ± 1	2 ± 0	–	–
	KB85	360	0.05 ± 0.00	36 ± 0	–	–	–
		360 + VRP[b]	0.10 ± 0.00	43 ± 0	43 ± 0	0.04 ± 0.00	170 ± 7
		180	0.04 ± 0.00	25 ± 0	–	–	–
	KBV1	360 + VRP[b]	0.06 ± 0.00	66 ± 1	1 ± 1	–	–

[a] Nonlinear least squares fits to eq 2 in Materials and Methods. Values shown are taken from fits to the average of at least three transients, with errors representing the computed error in the fitting parameters. [b] VRP = 10 μM verapamil. [c] A dash indicates that these parameters were not necessary to fit the data.

The entry of $DiOC_2(3)$ into both KB31 and KB85 is similar to that observed with $DiOC_3(3)$, in that the primary distinction for the two lines is the amplitude of the signal change and not the rate constants for entry. However, the redistribution characterized by k_2 in KB31 is absent from KB85 cells. While the amplitudes of accumulation of $DiOC_2(3)$ into KB31 are proportional to external dye concentration, they are not for accumulation into KB85, suggesting a saturable process of drug entry.

Incubation of KBV1 cells with $DiOC_2(3)$ and $DiOC_3(3)$ led to negligible signal changes from the background fluorescence of the external dye solution. There was no detectable entry of $DiOC_2(3)$ and $DiOC_3(3)$ into KBV1 cells, even at external dye concentrations of up to 900 nM. Thus, even during the initial 5 s of incubation, no $DiOC_2(3)$ or $DiOC_3(3)$ could be detected to associate with KBV1 cells.

Accumulation Determined by Cell Pelleting. The resulting amplitudes for the accumulation studies (Table 2) suggest that as pgp content increases, the amount of $DiOC_n(3)$ accumulated decreases, and this is in turn a function of alkyl chain length of the $DiOC_n(3)$. However, with fluorescent probes it is often difficult to relate signal intensity to absolute concentration due to the environmental dependence of the quantum yield. By pelleting the cells after steady-state levels had been reached, the quantity of dye associated with the cells was determined. This is shown in Figure 3, where the amount of accumulated dye is plotted as a percentage of external dye concentration. With $DiOC_7(3)$, all three cell lines accumulate approximately the same amount of dye. $DiOC_6(3)$ is accumulated to the same degree in KB31 and KB85 cells but is slightly reduced in KBV1. $DiOC_5(3)$

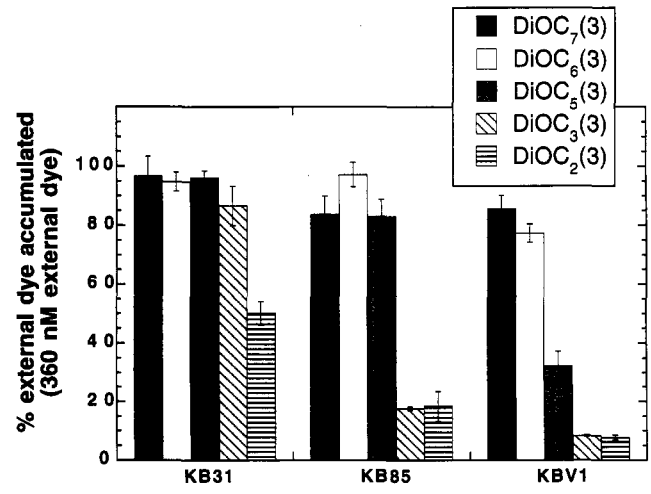

FIGURE 3: Accumulation of $DiOC_n(3)$ into KB cell lines determined by cell pelleting. As in Figure 2, when steady-state levels of dye accumulation had been reached, the cells were pelleted at 400*g*, and the pellet was resuspended in 2 mL of methanol to determine dye incorporation. Data shown are the average of triplicate determinations.

appears to be accumulated in a manner inversely proportional to pgp content. Little $DiOC_3(3)$ or $DiOC_2(3)$ was found to be associated with the KBV1 pellet, in agreement with the spectrometer measurements. The accumulation of these two dyes was also significantly reduced in KB85 cells as compared to KB31. The agreement between the amount of $DiOC_n(3)$ accumulation determined by cell pelleting and the amplitudes for process 1 and process 2 reported in Table 2 suggests that the amplitudes can, with some caution, be considered to represent concentration of dye entering the cells by process 1 and process 2.

Efflux of $DiOC_n(3)$. The rates of $DiOC_n(3)$ efflux and their dependence on pgp content were directly measured. Figure 4 shows the change in signal occurring with time for each $DiOC_n(3)$. The signal arising from the dye-containing cells is plotted relative to the initial signal from the cell suspension.

The efflux of $DiOC_{2-5}(3)$ from the KB cells could be modeled as either one or two simple exponential decays. The reduced cellular retention of $DiOC_n(3)$ in KB85 and KBV1 cells was fit following subtraction of $DiOC_n(3)$ efflux from KB31 cells under the same conditions. The parameters for the resulting fits are recorded in Table 3.

There was negligible efflux of both $DiOC_7(3)$ and $DiOC_6(3)$ from all three KB cell lines. The total signal change for efflux of these dyes was $\leq 10\%$ of their initial signal, and this minor change likely represents dye adhered to the plasma membrane and its subsequent release into the buffer. For KB31 cells, $DiOC_5(3)$ is also not effluxed to any extent. However, with the pgp-expressing KB85 cells, approximately 20% of the initial dye signal was effluxed over the first 400 s, followed by a steady signal. This efflux could be fit with a single exponential (Table 3). With highly pgp-expressing KBV1 cells, approximately 30% of the initial signal was lost after 400 s, with a slower efflux continuing to the end of the experiment. This process required two exponentials to effectively fit the data (Table 3). One exponential process corresponded to that observed in KB85 cells, with a second exponential of approximately the same amplitude but 5−10 times slower being necessary to fit the data.

The presence of pgp greatly affected the efflux of $DiOC_3(3)$. Some efflux of this dye occurred with KB31 cells, suggesting that their lower degree of hydrophobicity makes them more likely to diffuse from the cells into the surrounding buffer, even in the absence of pgp. However, in the KB85 cells, $DiOC_3(3)$ was effluxed to a marked degree relative to the $DiOC_{5-7}(3)$. The efflux of $DiOC_2(3)$ from pgp-expressing cells was also facilitated compared to the sensitive KB31 line. In KB85 cells, the $DiOC_2(3)$ signal fell to ~30% of its initial value by the end of the experiment. In the absence of verapamil, no $DiOC_2(3)$ or $DiOC_3(3)$ could be accumulated into KBV1, and therefore no efflux of these dyes could be measured.

Subcellular Distribution and Transport of $DiOC_n(3)$. In some cases, it has been shown that hydrophobic drug analogs are capable of circumventing pgp by altering their subcellular distribution (Lothstein et al., 1992a,b, 1993, 1994). Using fluorescence digital imaging microscopy, we have been able to track both the content and distribution of $DiOC_n(3)$ in KB85 cells and thus can determine whether altered distribution is responsible for the reduced pgp dependence on the transport properties of $DiOC_{6-7}(3)$. The accumulation and efflux of 10 nM $DiOC_2(3)$ and $DiOC_6(3)$ in individual pgp-expressing KB85 cells are shown in Figures 5 and 6. At these low concentrations, the background fluorescence of the dyes in the microscope image is minimized, and the signal arising in the field is exclusively due to dye accumulation within cells. The mitochondria of the cells are intensely stained by both dyes and are the primary organelles responsible for the enhanced fluorescence of the dyes. Both dyes stain perinuclear mitochondrial regions most intensely, and there is little alteration in the staining patterns from either dye. Thus, altered subcellular distributions of $DiOC_6(3)$ versus $DiOC_2(3)$ were not detected.

The efflux of each dye from the KB85 cells is quite different. After incubation in dye-free buffer, the $DiOC_2(3)$ is rapidly removed from the cells (Figure 6). The dye leaves all organelles and mitochondria at approximately the same rate and thus reflects a general lowered cellular concentration of dye. This efflux could be inhibited by including 10 μM verapamil in the efflux buffer (data not shown). The quantitative ability of FDIM allows calculation of the single-cell time course for efflux (Figure 7). After 1 h following change of media, the fluorescence from the $DiOC_2(3)$-stained cell is reduced almost 100% from its steady-state signal. This is in sharp contrast to $DiOC_6(3)$, which does not appear to be effluxed to any large extent from the individual KB85 cells (Figure 5). These data are in agreement with that obtained in the fluorescence spectrometer and further indicate the inability of pgp to mediate the retention of $DiOC_6(3)$ even though it is distributed intracellular to the same locations as $DiOC_2(3)$. Similar experiments with KB31 cells indicated that neither $DiOC_6(3)$ nor $DiOC_2(3)$ is distributed differently in the drug-sensitive line nor are the two dyes effluxed to any great extent from this cell line (data not shown).

Modulation of pgp Function by Verapamil. Results from both the fluorometer and FDIM experiments suggested that cellular transport of $DiOC_{6-7}(3)$ was not influenced by levels of pgp expression, although pgp-expressing cells were still resistant to the toxicity of these dyes in 7-day colony formation assays. It was therefore of interest to determine whether a pgp modulator such as verapamil could reverse resistance to the $DiOC_n(3)$ and also whether verapamil influenced the kinetics of transmembrane flux of the $DiOC_n(3)$.

Effect of Verapamil on $DiOC_2(3)$ and $DiOC_7(3)$ Toxicity. The 7-day toxicities of $DiOC_2(3)$ and $DiOC_7(3)$ were examined with the three cell lines in the continual presence of 10 μM verapamil. Verapamil did not affect the toxicity of the dyes to KB31 cells. In KB85, verapamil completely reversed resistance to $DiOC_7(3)$ and partially reversed resistance to $DiOC_2(3)$ (from 22-fold to 5-fold; IC_{50} + VRP = 0.26 ± 0.05 μM). In KBV1, verapamil partially reversed $DiOC_7(3)$ resistance (from 42-fold to 4-fold; IC_{50} + VRP = 0.22 ± 0.07 μM) and partially reversed $DiOC_2(3)$ resistance (from 73-fold to 6-fold; IC_{50} + VRP = 0.30 ± 0.03 μM).

Effects of Verapamil on $DiOC_n(3)$ Accumulation. The accumulation of $DiOC_7(3)$, $DiOC_5(3)$, $DiOC_3(3)$, and $DiOC_2(3)$ was repeated at 360 nM external dye concentration in the continual presence of 10 μM verapamil. The resulting accumulation profiles are given in Figure 8, and the parameters describing the curves are recorded in Table 2 (denoted by +VRP). In the case of $DiOC_7(3)$, very little difference in accumulation was observed in the presence of verapamil. The primary effect is a slight reduction of the amplitudes of accumulation and minor alterations of k_3, suggesting that the major effect of verapamil is to perturb subcellular trafficking of $DiOC_7(3)$. However, overall there

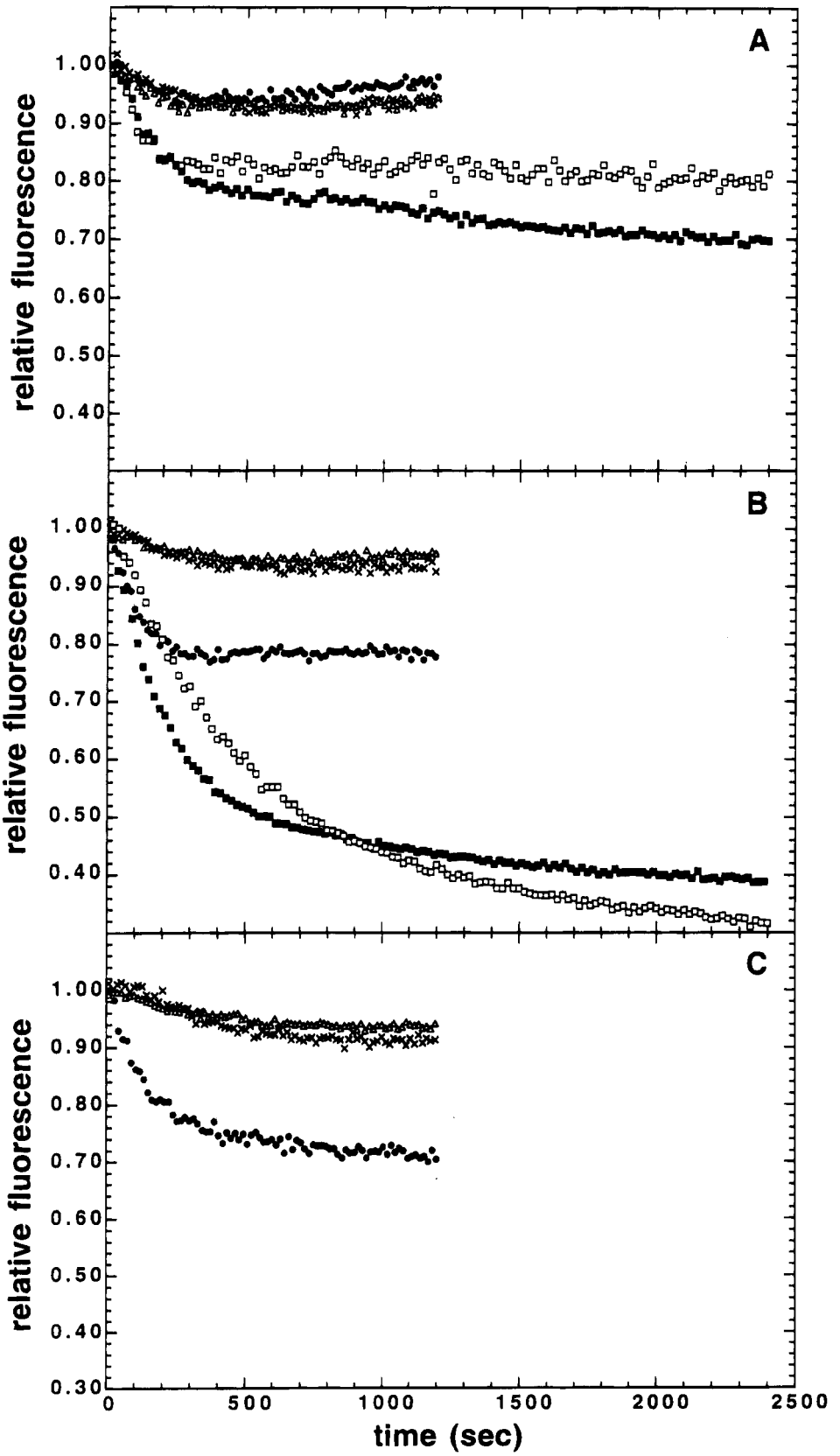

FIGURE 4: Efflux of $DiOC_n(3)$ from KB cell lines. Under the conditions shown in Figure 2 (360 nM dye external, 3×10^5 cells/mL), after steady-state levels had been achieved, the cells were pelleted at 400*g* and resuspended in 2 mL of dye-free buffer. Data are plotted relative to the initial signal from the resuspended cells. For $DiOC_{5-7}(3)$, only every third data point is plotted, while for $DiOC_{2-3}(3)$, every other data point is plotted. Plots are the average of at least three transients and show efflux of $DiOC_7(3)$ (△), $DiOC_6(3)$ (×), $DiOC_5(3)$ (●), $DiOC_3(3)$ (■), and $DiOC_2(3)$ (□) from (A) KB31, (B) KB85, and (C) KBV1 cells.

were no substantial differences in the accumulation profile, irrespective of the presence of pgp.

The effect of verapamil on $DiOC_5(3)$ accumulation was similar to that for $DiOC_7(3)$, in that the primary effect of the drug was to alter rate constants k_2 and k_3, which are related to intracellular trafficking of the drugs. In KB31 and KB85, the amplitudes of the signals arising from both process 1 and process 2 in the presence of verapamil were virtually

Table 3: Kinetic Parameters for Cellular $DiOC_n(3)$ Efflux[a]

dye	cell line	external concn (nM)	A_1 (relative)	$k_{-1} \times 10^4$ (s^{-1})	A_2 (relative)	$k_{-2} \times 10^4$ (s^{-1})
$DiOC_5(3)$	KB85	360	0.18 ± 0.01	91 ± 4	–[c]	–
		180	0.16 ± 0.02	153 ± 8	–	–
		360 + VRP[b]	none	–	–	–
	KBV1	360	0.15 ± 0.01	136 ± 17	0.20 ± 0.01	10 ± 3
		180	0.18 ± 0.01	175 ± 21	0.12 ± 0.01	26 ± 4
		360 + VRP[b]	–	–	0.08 ± 0.00	39 ± 4
$DiOC_3(3)$	KB85	360	0.32 ± 0.00	38 ± 1	–	–
		360 + VRP[b]	none	–	–	–
	KBV1	360 + VRP[b]	0.41 ± 0.02	87 ± 5	–	–
$DiOC_2(3)$	KB85	360	0.70 ± 0.00	19 ± 0	–	–
		180	0.54 ± 0.00	26 ± 0	–	–
		360 + VRP[b]	none	–	–	–
	KBV1	360 + VRP[b]	0.51 ± 0.00	25 ± 1	–	–

[a] Nonlinear least squares fits to single or double exponential efflux. The efflux from the drug-sensitive KB31 cell line was subtracted from the KB85 or KBV1 efflux curves prior to fitting the data. Values are taken from fits to the average of at least three transients, with errors representing the computed errors in the fitting parameters. [b] VRP = in the continuous presence of 10 μM verapamil. [c] A dash indicates that these parameters were not necessary to fit the data.

identical to those found in its absence. The effect on k_2 and k_3 in KB31 cells was modest; however, the values for k_2 and k_3 were significantly reduced in KB85 in the presence of verapamil. For KBV1 cells, addition of verapamil enhanced the amplitude of process 1 to near that of the KB85 and KB31 cells, indicating a correcting of accumulation defects in this cell line. However, the accumulation of $DiOC_5(3)$ into KBV1 in the presence of verapamil could now be described by a simple two-exponential accumulation process.

Interestingly, the effects on $DiOC_3(3)$ accumulation by verapamil are in marked contrast to those observed with $DiOC_5(3)$. In the case of $DiOC_3(3)$, the effect of verapamil is to enhance k_1, while having a much less pronounced effect on k_2 or k_3. Furthermore, the amplitudes for accumulation of $DiOC_3(3)$ into KB31 and KB85 are approximately the same in the presence of verapamil, indicating that the two cell lines now accumulate the same amount of dye. Importantly, the addition of verapamil also allows the accumulation of $DiOC_3(3)$ into KBV1 to be detected, whereas no accumulation appears to occur in the absence of verapamil. The parameters that describe the entry of $DiOC_3(3)$ into KBV1 are quite different from those obtained for KB31 or KB85 in either the presence or absence of verapamil.

As with $DiOC_5(3)$, the effect of verapamil on accumulation of $DiOC_2(3)$ is primarily to affect the amplitudes of the signals observed and the values for k_2. The values for k_1 are similar in the KB31 and KB85 cell lines ± verapamil, but the value for k_2 is increased in the presence of verapamil. $DiOC_2(3)$ can also be accumulated into KBV1 in the presence of verapamil, and the accumulation kinetics are very similar to that observed for $DiOC_2(3)$ in KB31 (minus verapamil).

Effect of Verapamil on $DiOC_n(3)$ Efflux. As in the absence of verapamil, inclusion of 10 μM verapamil in the efflux experiments resulted in no efflux of $DiOC_6(3)$ or $DiOC_7(3)$ from any of the KB cell lines. However, this concentration of verapmil did almost completely inhibit the efflux of $DiOC_5(3)$ from KB85 (Figure 9C; Table 3). Verapamil also eliminated one of the efflux components from KBV1 cells. However, the second component of efflux was still present, albeit to a lesser degree (Figure 9C; Table 3).

When verapamil was present in the buffer, there was complete inhibition of efflux of $DiOC_3(3)$ from KB85 cells (Figure 9B). Further, when verapamil was used, there was detectable accumulation of $DiOC_3(3)$ into KBV1 (Table 2). The subsequent efflux of this dye from the KBV1 cells was examined in the continual presence of verapamil (Figure 9B). Efflux of $DiOC_3(3)$ could not be prevented by verapamil, and the resulting single exponential decay had a rate constant 2−3-fold higher than that found for KB85 in the absence of verapamil.

Loading of KBV1 cells with $DiOC_2(3)$ could also be accomplished using verapamil. As seen with $DiOC_3(3)$, the efflux of $DiOC_2(3)$ from loaded KBV1 cells could not be inhibited by 10 μM verapamil (Figure 9A), and the cells cleared most of the dye by the end of the experiment. Thus, the efflux mechanism for both $DiOC_2(3)$ and $DiOC_3(3)$ in KBV1 cells is maintained by KBV1 at 10 μM verapamil, a concentration that is able to only partially reverse pgp-mediated resistance to $DiOC_2(3)$ in this cell line.

DISCUSSION

Using $DiOC_n(3)$ derivatives, we have examined the effect of a simple structural modification on the ablity of compound to be a substrate for pgp. The fluorescence of $DiOC_n(3)$ is increased dramatically as the dyes enter the cells and thus provides a mechanism for monitoring influx, efflux, and subcellular distribution of the dyes as a function of their increasing hydrophobic tails. These studies provide an added dimension to existing MDR cellular transport studies in that they probe the accumulation and efflux of cytotoxic compounds into/from MDR cells at up to 1.5-s resolution. Importantly, we are able to monitor the initial, immediate interaction of the dyes with pgp-expressing cells.

Our results have produced several clues in understanding the function of pgp as a cellular protection mechanism. We have found that, within a given series of similar structures, the effectiveness of pgp-expressing cells to efflux toxic compounds is inversely proportional to their hydrophobicity. Furthermore, the drug resistance of pgp-expressing cells may occur without altering either the subcellular distribution of toxin or the membrane transport properties of the toxin.

The toxicity studies described in Table 1 clearly indicate that all the $DiOC_n(3)$ dyes are part of the MDR phenotype, in that increasing expression of pgp in three KB cell lines leads to increased resistance to the toxicity of the dyes. This is in agreement with previous studies using $DiOC_2(3)$ (Chaudhary & Roninson, 1991) and $DiOC_5(3)$ (Crifo et al., 1991). The utility of the $DiOC_n(3)$ over other compounds known to be part of the MDR phenotype is the environmental

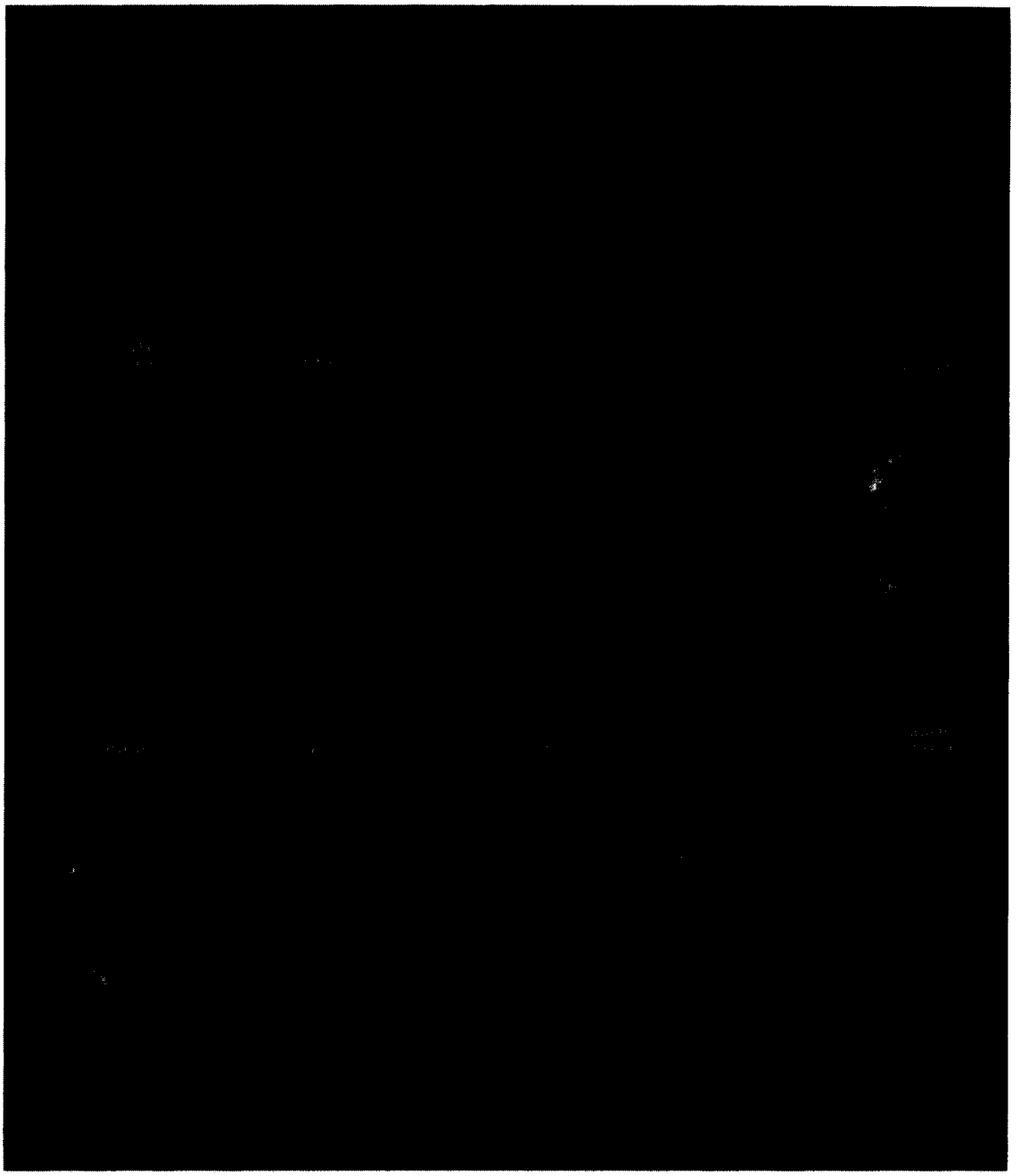

FIGURE 5: Accumulation and efflux of $DiOC_6(3)$ in single KB85 cells. The fluorescence from a field of cells was monitored upon incubating them with 10 nM $DiOC_6(3)$. Accumulation and/or efflux was followed for the indicated time. The efflux of $DiOC_6(3)$ was measured by replacing the incubation media with dye-free buffer ("wash"). $DiOC_6(3)$ stained primarily the mitochondria and was poorly effluxed from the cells. Data shown are representative of three experiments.

sensitivity of their fluorescence. Using the accumulation mechanism outlined in eqs 1−3, we can distinguish the effect of pgp expression on $DiOC_n(3)$ transport, how this relates to the toxicity of the dye, and additionally, how the inclusion of verapamil (a compound known to reverse the effects of pgp expression) affects the transport of the dyes. The model we have used is effective in describing the accumulation of all $DiOC_n(3)$. However, the effective rate constants are generally different among the dyes. This is likely due to the fact that different $DiOC_n(3)$'s have been noted to stain different organelles in addition to mitochondria (Haugland, 1992) and thus each dye may be accumulated by a different pathway. For a given dye, the values for k among cell lines are fairly consistent, providing a basis for comparing the mechanism of dye accumulation and the effect of verapamil on this mechanism.

Some surprising findings have emerged from our studies. In opposition to the often proposed mechanism of pgp as an "efflux pump" for toxins, we find that pgp expression and "transport" of toxins are not necessarily correlated. An illustration of this statement is the $DiOC_7(3)$ dye. The KB85 cell line, which moderately overexpresses pgp, is 7-fold resistant to the toxicity of the compound relative to the parent KB31 line, while the KBV1 cells, which greatly overexpress pgp, are 42-fold resistant to the dye. When the transport properties of $DiOC_7(3)$ were examined, we found that all three cell lines accumulated dye to approximately the same steady-state levels and, more importantly, that the mechanism of dye accumulation, as defined by influx kinetic parameters, was virtually identical in the three cell lines (Table 2). Furthermore, there was no significant efflux of the accumulated $DiOC_7(3)$, even in the highly resistant KBV1 line.

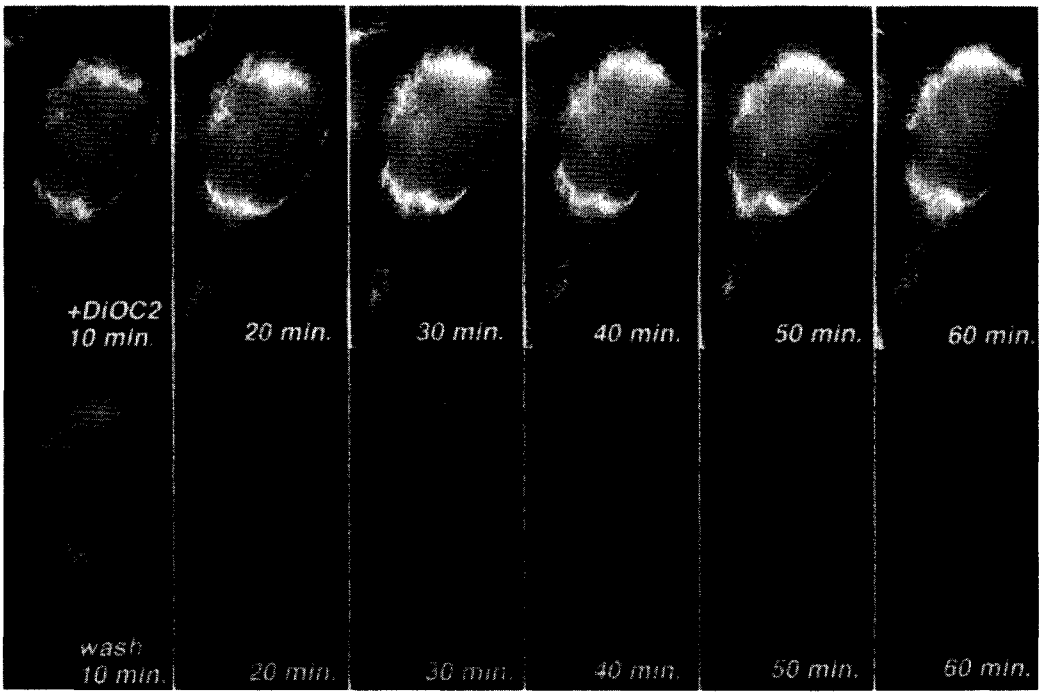

FIGURE 6: Accumulation and efflux of $DiOC_2(3)$ in a single KB85 cell. The fluorescence from a field of cells was monitored upon incubating them with 10 nM $DiOC_2(3)$. Accumulation and/or efflux was followed for the indicated time. Efflux was measured by replacing the incubation media with dye-free buffer (wash). The $DiOC_2(3)$ stained primarily the mitochondria of the cells and was effectively effluxed from all locations within the cell simultaneously. This efflux could be inhibited by addition of 10 μM verapamil. Data shown are representative of three experiments.

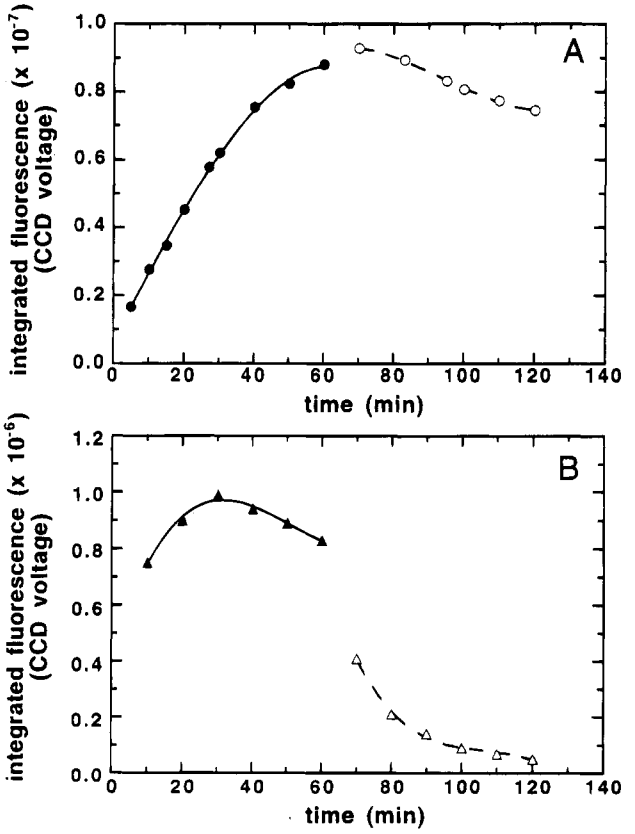

FIGURE 7: Quantitation of accumulation and efflux of $DiOC_6(3)$ and $DiOC_2(3)$ in KB85 cells. The digital images in Figures 5 and 6 were quantitiated by subtracting an appropriate background and integrating the fluorescence from the entire image. Panels: (A) accumulation (●) and efflux (○) of $DiOC_6(3)$ in KB85; (B) accumulation (▲) and efflux (△) of $DiOC_2(3)$ in KB85.

The transport parameters were not significantly affected by the presence of verapamil in any of the cell lines. These data indicate that drug resistance, although proportional to pgp content, does not depend on the transport of the $DiOC_7(3)$ by pgp.

With $DiOC_6(3)$, slight differences in parameters can be observed with increasing pgp levels. KB85 and KBV1 cells exhibit decreased amplitudes in process 1 and process 2 of drug accumulation as compared to KB31, as well as slightly reduced rate constants for process 1. This suggests that pgp affects both the initial accumulation of $DiOC_6(3)$ and the manner with which it is trafficked intracellularly.

The presence of pgp is particularly noticeable in the accumulation of $DiOC_5(3)$, where the amplitude for dye accumulation by both process 1 and process 2 is significantly lowered, but the effect of pgp on the accumulation of this dye varies among cell lines. At higher external dye concentrations (360 nM), where reasonably high levels of internal dye concentrations are reached, the values for k_1 are consistent among cell lines. However, at these concentrations the values for k_2 are distinctly different in all three cell lines, while the k_3 values remain approximately constant ($\leq$2-fold in KB85). These data suggest that the action of pgp on $DiOC_5(3)$ is manifested after the dye has passed through the plasma membrane and occurs during redistribution of the dye within the cytoplasm and/or mitochondria. Inclusion of verapamil also appears to affect k_2 and k_3 and thus also affects cytoplasmic redistribution of dye. Importantly, these data suggest that a chain length of five carbons is effectively recognized by pgp in KBV1 cells but less so in KB85 cells.

$DiOC_3(3)$ and $DiOC_2(3)$ are accumulated much more slowly into both KB31 and KB85 cells than the $DiOC_n(3)$ bearing longer chains. This is likely due to the decreased lipophilicity of these dyes as compared to the other $DiOC_n(3)$, as reported for the chain-length dependence of $DiOC_n(3)$ penetration of phospholipid bilayers (Waggoner et al., 1975). The presence of pgp in the KB85 cell line did not significantly affect the rate constants associated with $DiOC_3(3)$ influx, affecting only the amplitude of the signal

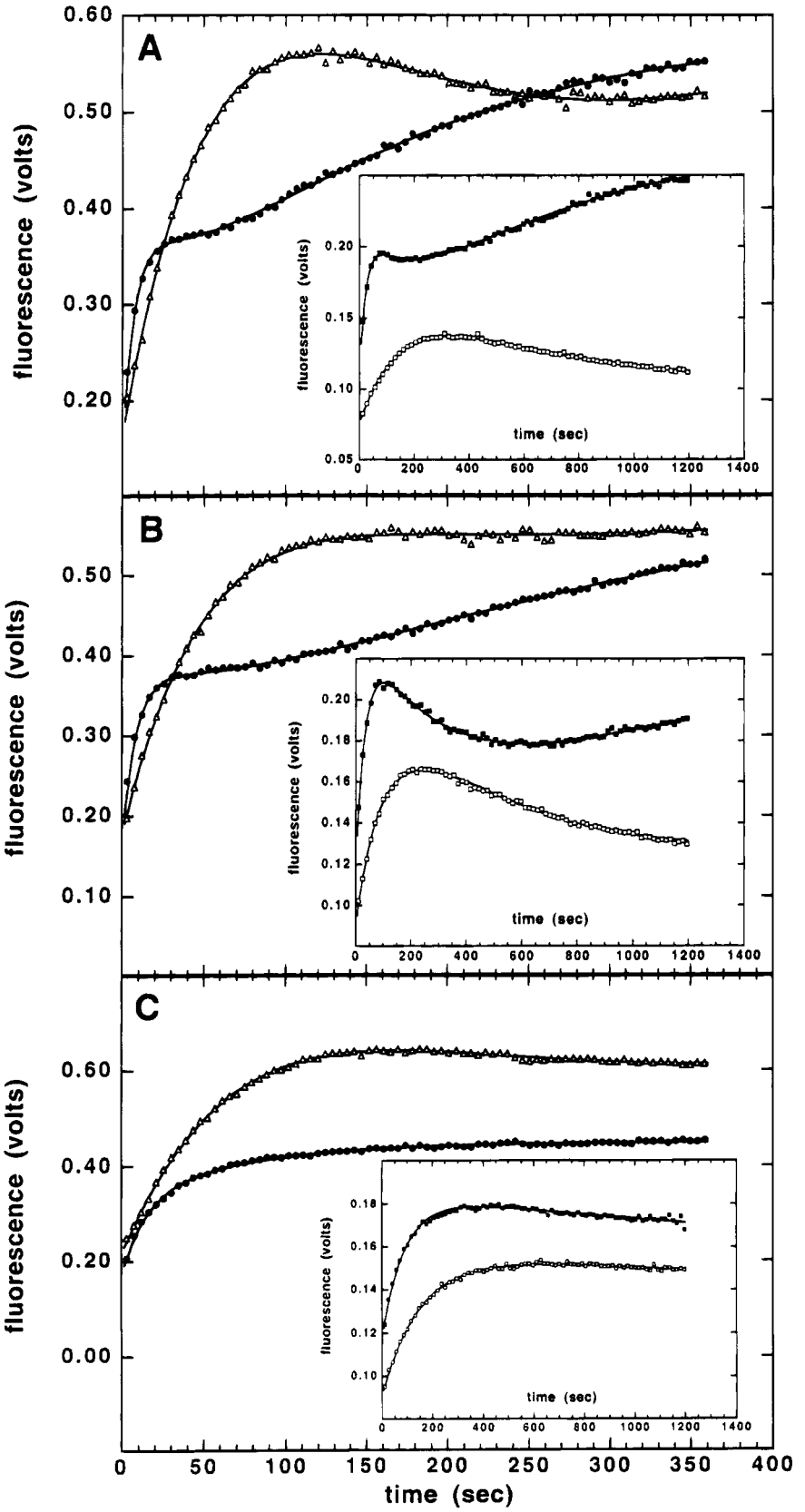

FIGURE 8: Accumulation of $DiOC_n(3)$ into KB cell lines in the presence of 10 μM verapamil. For clarity of presentation, only every third data point is plotted for $DiOC_{5-7}(3)$, while every other data point is plotted for $DiOC_{2-3}(3)$. Solid lines represent curve fits to eq 2 or 3 in Materials and Methods. The resulting parameters are recorded in Table 2. Plots are the average of at least three transients and show accumulation of 360 nM external $DiOC_7(3)$ (△), $DiOC_5(3)$ (●), $DiOC_3(3)$ (■), and $DiOC_2(3)$ (□) into 3×10^5 cells/mL (A) KB31, (B) KB85, and (C) KBV1 cells.

change. With $DiOC_2(3)$ the presence of pgp in KB85 cells seems to completely eliminate the redistribution aspect of process 1 of the accumulation of this dye (i.e., the amplitude of the contribution of the $B \rightarrow C$ step falls to approximately zero), and the accumulation can be described by a single exponential function ($A \rightarrow B$). As mentioned earlier, no detectible amounts of $DiOC_2(3)$ or $DiOC_3(3)$ could be accumulated into KBV1 cells (i.e., amplitudes fall to zero).

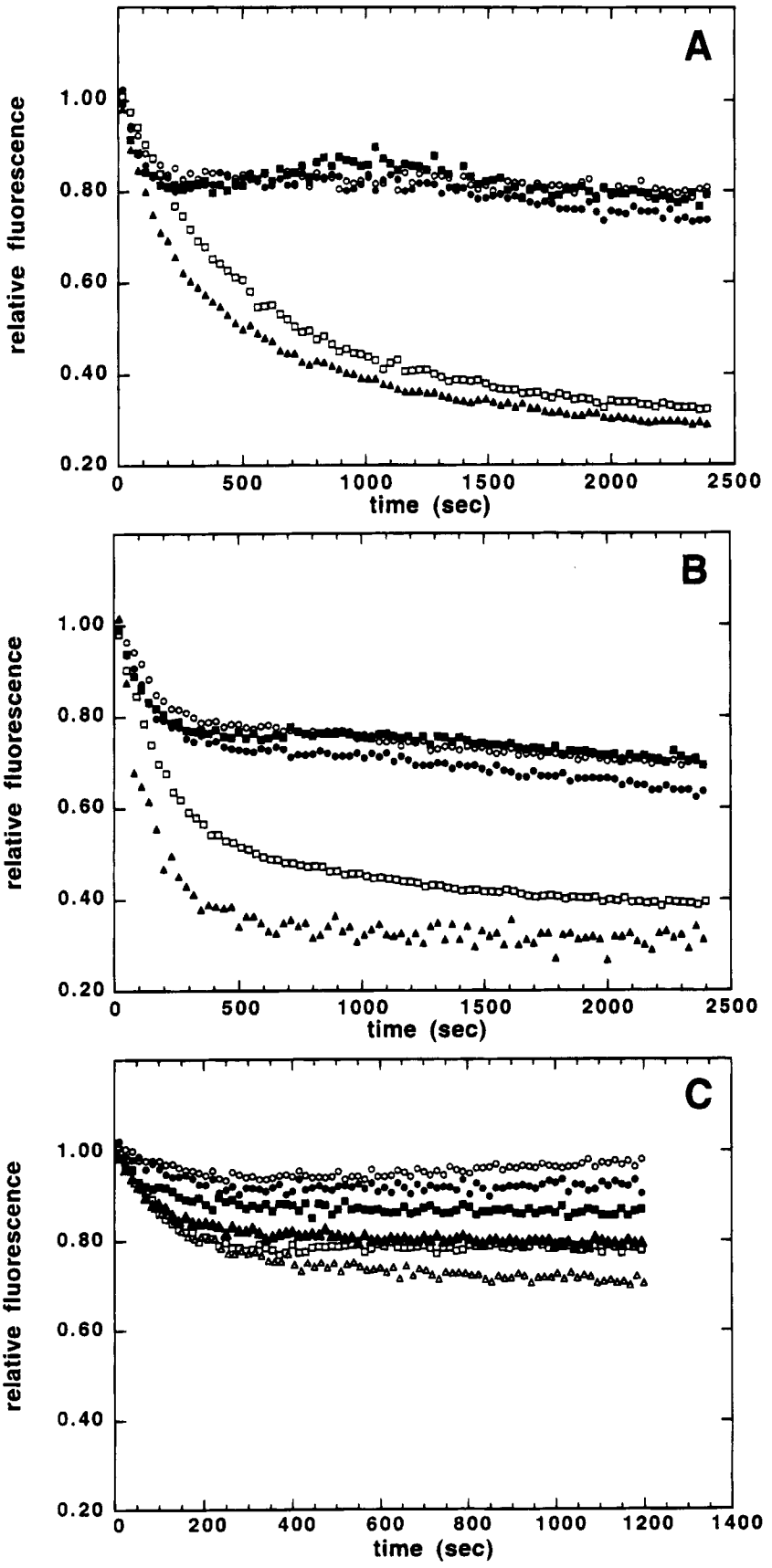

FIGURE 9: Effect of verapamil on efflux of $DiOC_n(3)$ from KB cell lines. Under the conditions shown in Figure 4 (360 nM dye external, 3×10^5 cells/mL), after steady-state levels had been achieved, the cells were pelleted at 400*g* and resuspended in 2 mL of dye-free buffer ± verapamil. Data are plotted relative to the initial signal from the resuspended cells. Only every third data point is plotted. Plots are the average of at least three transients. Panels: (A) $DiOC_2(3)$ efflux from KB31 (○), KB31 + 10 μM verapamil (●), KB85 (□), KB85 + 10 μM verapamil (■), and KBV1 + 10 μM verapamil (▲); (B) $DiOC_3(2)$ efflux from KB31 (○), KB31 + 10 μM verapamil (●), KB85 (□), KB85 + 10 μM verapamil (■), and KBV1 + 10 μM verapamil (▲); (C) $DiOC_5(3)$ efflux from KB31 (○), KB31 + 10 μM verapamil (●), KB85 (□), KB85 + 10 μM verapamil (■), KBV1 (△), and KBV1 + 10 μM verapamil (▲).

The presence of verapamil affected k_1 for accumulation of $DiOC_3(3)$ into all three cell lines but did not substantially alter k_2 or k_3. This implies that verapamil facilitates initial entry of the dye into the cells but does not affect subcellular redistribution. This is in contrast to the effect seen with $DiOC_2(3)$, where the value for k_2 is affected by verapamil but not k_1. These results indicate that, even in a simple system of compounds such as the $DiOC_n(3)$, the addition of another compound such as an MDR modulator can greatly affect subcellular transport of the dye of interest. It should be noted that even in the sensitive KB31 line the verapamil-induced alteration of dye accumulation pathways was observed, suggesting that effects other than a direct inhibition of pgp are occurring.

In summary, the accumulation data lead to a picture of pgp as a protein that alters subcellular distribution pathways for hydrophilic $DiOC_n(3)$ once they have initially entered the cell. This does not mean that the $DiOC_n(3)$'s bind to altered subcellular targets (Figures 5 and 6) but rather that the paths leading to these targets are altered in MDR cells. It is difficult to interpret the nature of the subcellular rerouting of $DiOC_{5-7}(3)$ due to the high degree of lipophilicity of these compounds. However, the trend to affect subcellular distribution rate constants can be seen even with these dyes (Table 2). The effect of pgp on the more hydrophilic $DiOC_{2-3}(3)$ is more straightforward and indicates that pgp alters the amount of dye entering the cell without altering the membrane permeability of the cell. This important conclusion has been suggested in earlier experiments where direct rates of dye accumulation have been measured (Ramu et al., 1989; Roepe, 1992).

The efflux data contain further proof of the lack of correlation of transport properties with toxicity, particularly if one considers the toxicities of the $DiOC_n(3)$ within a given cell line. $DiOC_5(3)$ and $DiOC_7(3)$ show marked differences in their retention in pgp-expressing cells. KBV1 cells efflux $DiOC_5(3)$ much more effectively than $DiOC_7(3)$ (Figure 4), and accumulation of $DiOC_5(3)$ is significantly altered as compared to $DiOC_7(3)$ (Figures 2 and 3). The $DiOC_5(3)$ efflux could be inhibited with verapamil, making it a "classic" pgp substrate [e.g., Tsuruo et al. (1981) and Cornwell et al. (1987)]. However, the two dyes show almost identical toxicities for 7-day exposure (Table 1). This is further elaborated by comparing the toxicity of $DiOC_7(3)$ and $DiOC_3(3)$ in KB85. $DiOC_3(3)$ appears to be substantially effluxed by the KB85 cells (Figure 4), and this efflux can be inhibited by verapamil. Although $DiOC_7(3)$ is not effluxed at all, it has an identical 7-day toxicity in the KB85 lines as $DiOC_3(3)$. Thus, we conclude that pgp-dependent transport of $DiOC_n(3)$ dyes is not mirrored in their cytotoxic activity, although pgp expression does result in differences in toxicity from the parent cell line. For both KB85 and to a greater extent KBV1, this implies that resistance due to pgp may be superimposed on other cellular resistance mechanisms, and thus the lack of a structure-based understanding of substrates for pgp may be due to other modes of resistance, even in cells that overexpress pgp. This notion is further supported by the efflux of $DiOC_n(3)$ from KBV1 cells, in which an efflux mechanism, poorly inhibited by verapamil, is superimposed on a verapamil-sensitive efflux.

The fact that pgp-mediated resistance to $DiOC_7(3)$ can be reversed (either partially or fully) by incubation with verapamil might carry the implication that verapamil interacts with pgp to prevent the transport of $DiOC_7(3)$ from the resistant cell lines. However, our measurements of cellular flux of $DiOC_7(3)$ in pgp-expressing cells indicate that this process is almost completely unaffected by verapamil, suggesting that pgp is not involved in the membrane permeability of $DiOC_7(3)$. In this context, our data imply that verapamil may function to reverse drug resistance at a locus distinct from pgp.

Alternatively, our studies may indicate that short-term measurements of membrane transport properties, as have been measured in virtually all studies to date of pgp-mediated transport, may not be linked to long-term (5−7 day) cell survival. This is in spite of the fact that our accumulation/efflux measurements were performed at concentrations of dye close to the IC_{50} for the cell lines being examined. These results may explain at least part of the difficulty in identifying drug structure−activity relationships in pgp-expressing cells.

Interestingly, there seems to be a critical chain length of 5 carbons that distinguishes whether or not a compound is recognized (through alterations in influx and efflux properties) by pgp. This is, in a sense, in agreement with work done using both alkylpyridiniums (Dellinger et al., 1992) and alkylated anthracycline derivatives (Lothstein et al., 1994). However, in the alkylpyridinium experiments, it was found that a 5-carbon chain was needed for pgp recognition, whereas Lothstein and co-workers found that this chain length was able to circumvent pgp. However, with the $DiOC_n(3)$ there is no dependence of chain length on toxicity in KB85 cells. Since it appears that an electron-delocalized ring system is important for pgp recognition (Dellinger et al., 1992), the fact that the anthracyclines and the $DiOC_n(3)$ both have extended ring systems as compared to alkylpyridiniums may, in some fashion, be responsible for this difference. However, our results with KB85 cells suggest the $DiOC_n(3)$ toxicities are more like the alkylguanidiniums studied by Dellinger et al., in that those compounds also showed no length-dependent toxicity to sensitive vs resistant cell lines.

The origins of the tail length dependence of pgp "recognition" may be in the differential response to membrane potentials that occur with $DiOC_n(3)$. These dyes are among a group of hydrophobic cationic compounds that have been used to measure membrane potentials in a variety of cell types (Sims et al., 1974; Waggoner, 1979). The mechanism of this measurement is that increased membrane potential results in increased cell-associated dye, which in turn results in altered dye fluorescence. Sims et al. (1974) have shown that, in the $DiOC_n(3)$ series, $DiOC_6(3)$−$DiOC_8(3)$ show little or no response to valinomycin-induced membrane hyperpolarization, whereas $DiOC_2(3)$−$DiOC_5(3)$ do show a substantial response. This may be due to the fact that the longer alkyl chain dyes are significantly membrane bound, preventing true Nernstian distribution, and are therefore unable to accurately probe membrane potential. This problem is similar to that observed with rhodamine derivatives (Ehrenberg et al., 1988). The membrane association in the absence of a potential is much less for $DiOC_2(3)$ (Bunting et al., 1989) and presumably is similar for $DiOC_3(3)$.

Considering MDR cells to have decreased membrane potentials would explain the result that $DiOC_3(3)$ and $DiOC_2(3)$ could not be detected to enter KBV1 cells. We could detect no change in fluorescence with these two dyes even at external concentrations as high as 900 nM (data not shown), and thus the pgp pump could not be saturated. Pelleted KBV1 cells also were found to contain little or no

$DiOC_{2-3}(3)$. These results were highly surprising, considering the slow efflux of $DiOC_{2-3}(3)$ from KB85 cells, relative to their rates of accumulation (Figure 4, Table 3). These data imply that either $DiOC_{2-3}(3)$ does not enter KBV1 cells or that it is highly efficiently effluxed from the cells. This is, in part, also true with accumulation of $DiOC_5(3)$ in KBV1 cells, where only approximately 30% of the accumulated dye signal is available to be effluxed (Figure 4).

Our results may be interpreted by considering pgp as an ion-regulating protein, manipulating cell pH and/or membrane potential. This would explain why $DiOC_2(3)$ and $DiOC_3(3)$ could not be detected to enter KBV1 cells or why pgp action could not be saturated at concentrations of these dyes near 1 μM. Such a mechanism for pgp action has been described in several studies (Alabaster et al., 1989; Thiebaut et al., 1990; Roepe, 1992; Roepe et al., 1993; Simon et al., 1994). In support of this idea, Crifo et al. (1991) have shown that DOX-resistant MDR cells show pronounced accumulation of $DiOC_5(3)$ when hyperpolarized via valinomycin, in comparison to their drug-sensitive counterparts. The ion regulation by pgp would presumably be at the plasma membrane level, however, since $DiOC_7(3)$ is capable of equally staining the mitochondria of the three KB cell lines, suggesting that pgp expression does not significantly alter mitochondrial function.

As an alternative mechanism, it could also be argued that pgp transports the $DiOC_n(3)$ in some fashion, presumably by "binding" the drugs at the plasma membrane level. Although it is unnecessary to invoke such a mechanism to explain our results, it is conceivable that this scenario could give results similar to those observed here. However, with this type of model it would be difficult to explain how such a transporter could affect only the concentrations of accumulated dye without affecting membrane permeability [e.g., $DiOC_{2-3}(3)$ transport in KB31 vs KB85 cells].

Irrespective of the exact role of the protein, the data presented here suggest that the resistance to $DiOC_n(3)$ due to pgp expression does not correlate with the transport properties of the dyes. However, the presence of pgp results in a mechanism that reduces the steady-state levels (amplitudes) of dye accumulation while having significantly lesser effect on the rate constants for entry. Furthermore, pgp affects the transport of hydrophilic compounds to a greater extent than hydrophobic ones. Our results caution against directly attributing drug transport properties of structurally diverse compounds to the mechanism by which pgp protects cells and interpreting reversal of resistance by modulators as being a consequence of action at the pgp locus. Even in the case of structurally similar compounds such as the $DiOC_n(3)$ there are complex relationships between transport and toxicity.

ACKNOWLEDGMENT

The authors thank Elisha Jenkins for excellent technical assistance.

REFERENCES

Alabaster, O., Woods, T., Oritz-Sanchez, V., & Jahangeer, S. (1989) *Cancer Res. 49*, 5638−5643.

Beck, W. T., & Qian, X.-D. (1992) *Biochem. Pharmacol. 43*, 89−93.

Bunting, J. R. (1992) *Biophys. Chem. 42*, 163−175.

Bunting, J. R., Phan, T. V., Kamali, E., & Dowben, R. M. (1989) *Biophys. J. 56*, 979−993.

Chaudhary, P. M., & Roninson, I. B. (1991) *Cell 66*, 85−94.

Cornwell, M. M., Pastan, I., & Gottesman, M. M. (1987) *J. Biol. Chem. 262*, 2166−2170.

Crifo, C., Capuozzo, E., Cucco, C., Zupi, G., & Salerno, C. (1991) *Biochem. Int. 25*, 593−601.

Dellinger, M., Pressman, B. C., Calderon-Higginson, C., Savaraj, N., Tapiero, H., Kolonias, D., & Lampidis, T. J. (1992) *Cancer Res. 52*, 6385−6389.

Ehrenberg, B., Montana, V., Wei, M.-D., Wuskell, J. P., & Loew, L. M. (1988) *Biophys. J. 53*, 785−794.

Endicott, J. A., & Ling, V. (1989) *Annu. Rev. Biochem. 58*, 137−171.

Ford, J. M., & Hait, W. N. (1990) *Pharmacol. Rev. 42*, 155−199.

Gros, P., Talbot, F., Tang-Wai, D., Bibi, E., & Kaback, H. R. (1992) *Biochemistry 31*, 1992−1998.

Haugland, R. P. (1992) *Handbook of Fluorescent Probes and Research Chemicals*, Molecular Probes, Eugene, OR.

Horio, M., Gottesman, M. M., & Pastan, I. (1988) *Proc. Natl. Acad. Sci. U.S.A. 85*, 3580−3584.

Horio, M., Lovelace, E., Pastan, I., & Gottesman, M. M. (1991) *Biochim. Biophys. Acta 1061*, 106−110.

Horton, J. K., Houghton, J. A., & Houghton, P. H. (1990) *Proc. Am. Assoc. Cancer Res. 31*, 404.

Klopman, G., Srivastava, S., Kolossvary, I., Epand, R. F., Ahmed, N., & Epand, R. M. (1992) *Cancer Res. 52*, 4121−4129.

Lothstein, L., Sweatman, T. W., Dockter, M. E., & Israel, M. (1992a) *Cancer Res. 52*, 3409−3417.

Lothstein, L., Wright, H. M., Sweatman, T. W., & Israel, M. (1992b) *Oncol. Res. 4*, 341−347.

Lothstein, L., Hosey, L. M., Sweatman, T. W., Koseki, Y., Dockter, M., & Priebe, W. (1993) *Oncol. Res. 5*, 229−234.

Lothstein, L., Rodrigues, P. J., Sweatman, T. W., & Israel, M. (1994) *Proc. Am. Assoc. Cancer Res. 35*, 342.

McKenna, N. M., & Wang, Y.-L. (1989) *Methods Cell Biol. 29*, 195−205.

Moore, J. W., & Pearson, R. G. (1981) *Kinetics and Mechanism*, pp 290−296, John Wiley & Sons, New York.

Ramu, A., Pollard, H. B., & Rosario, L. M. (1989) *Int. J. Cancer 44*, 539−547.

Roepe, P. D. (1992) *Biochemistry 31*, 12555−12564.

Roepe, P. D., Wei, L.-Y., Cruz, J., & Carlson, D. (1993) *Biochemistry 32*, 11042−11056.

Seligmann, B. E., & Gallin, J. I. (1983) *J. Cell. Physiol. 115*, 105−115.

Shalinsky, D. R., Jekunen, A. P., Alcaraz, J. E., Christen, R. D., Kim, S., Khatibi, S., & Howell, S. B. (1993) *Br. J. Cancer 67*, 37−46.

Shen, D.-W., Cardarelli, C., Hwang, J., Cornwall, M., Richert, N., Ishii, S., Pastan, I., & Gottesman, M. M. (1986) *J. Biol. Chem. 261*, 7762−7770.

Simon, S., Roy, D., & Schindler, M. (1994) *Proc. Natl. Acad. Sci. U.S.A. 91*, 1128−1132.

Sims, P. J., Waggoner, A. S., Wang, C.-H., & Hoffman, J. F. (1974) *Biochemistry 13*, 3315−3330.

Sirotnak, F. M., Yang, C.-H., Mines, L. S., Oribè, E., & Biedler, J. L. (1986) *J. Cell. Physiol. 126*, 266−274.

Stein, W. D., Cardarelli, C., Pastan, I., & Gottesman, M. M. (1994) *Mol. Pharmacol. 45*, 763−772.

Stow, M. W., & Warr, J. R. (1993) *FEBS Lett. 320*, 87−91.

Tew, K. D., Houghton, P. J., & Houghton, J. A. (1993) in *Preclinical and Clinical Modulation of Anticancer Drugs*, pp 125−196, CRC Press, Boca Raton, FL.

Thiebaut, F., Currier, S. J., Whitaker, J., Haugland, R. P., Gottesman, M. M., Pastan, I., & Willingham, M. C. (1990) *J. Histochem. Cytochem. 38*, 685−690.

Tsuruo, T., Iida, H., Tsukagoshi, S., & Sakurai, Y. (1981) *Cancer Res. 41*, 1967−1972.

Wadkins, R. M., & Houghton, P. J. (1993) *Biochim. Biophys. Acta 1153*, 225−236.

Waggoner, A. A., Sirkin, D., Tolles, R., & Wang, C.-H. (1975) *Biophys. J. 15*, 20a.

Waggoner, A. S. (1979) *Annu. Rev. Biophys. Bioeng. 8*, 47−68.

BI942044O